232 Transaction of the Korean Society of Mechanical Engineers, Vol. 9, No. 2, pp. 232~239, 1985.

<Original>

Flooding and Hysteresis Effects in Nearly-Horizontal Two-Phase Countercurrent Stratified Flow

Sang Chun Lee*

(Received November 24, 1984)

근사수평 이상반류성층유동에서의 플러딩 및 히스테리시스효과

이 상 천

초 록

근사수평 이상반류유동에서의 플러딩천이에 대한 실험을 수행하였으며 이것을 바탕으로 반류유동도(flow-regime map)를 완성하였다. 또 플러딩천이에 대한 응축의 영향을 고찰하였는데 플러딩이 액체입구에서 야기될 때 플러딩 속도는 응축량을 고려한 유효증기량으로 표시되며 이 경우 반드시 히스테리시스효과를 동반하게 된다. 이 효과는 응축에 기인한는 것으로 그 메카니즘을 구명하였다. 또 전달액체유량이 영이 될때의 임계증기속도는 액체분출유량이나 액체서브쿠울링의 정도에 무관하며 본 연구에서 사용한 관의 경우, 수정 Wallis 변수로 1.74 로 나타났다.

Nomenclature

C_{pl} : Specific heat of liquid(kJ/kg°K)
f : Condensation efficiency
g : Gravitational acceleration(m/s²)
i_{fg} : Latent heat(kJ/kg)
j : Superficial velocity(m/s)
J_m^* : Modified Wallis parameter
Ja : Jacob number
L : Length scale(m)
T : Temperature(°C)

Greek Symbols

η : Dimensionless parameter
θ : Inclination angle
ρ : Density(kg/m³)

Subscripts

e : Effective
f : Liquid
g : Gas
k : k-phase(f or g)
in : Inlet
out : Outlet
s : Saturation

*Member, Marine Engineering Department Yeungnam University

1. Introduction

Flooding in countercurrent gas-liquid flow is an important phenomenon in a variety of industrial applications such as tubular reflux con-

densers, film separators and tubular contactors. Recently, considerable attention has been given to the flooding problem in connection with the safety analysis of nuclear reactor systems. Flooding may limit the penetration of emergency core coolant(ECC) into a hot reactor core either in the cold leg or in the downcomer of a pressurized-water reactor(PWR) during a postulated loss-of-coolant accident(LOCA). Significant effort has been devoted to improving the understanding of the flooding phenomena in conjunction with the performance of these nuclear reactor systems.[1,2]

One of important features of flooding is that tube-end geometries appear to be critical in determining the flooding velocity. Further, the end effects play a significant role in deciding the locus of initiation of flooding, which is of importance in a condensing flow. Condensation may not only alter the vapor flooding velocity but change the flooding characteristics during the partial delivery stage, depending upon the locus of the onset of flooding. It may cause a sudden reduction of the liquid delivery rate, called "hysteresis effects", once the flow is flooded. The hysteresis effects may also take place in an adiabatic two-phase countercurrent flow as reported by Wallis, et al.[3] presumably due to the breakup of a liquid film. but the occurrence of these effects appears to be dependent upon various experimental factors such as the tube-end geometry. However, the initiation and basic mechanisms of these hysteresis effects in a condensing flow as well as in an adiabatic flow have not been well understood yet.

Many previous studies of flooding have dealt with the prediction of the onset of flooding in vertical annular flow. However, flooding in horizontal, or nearly-horizontal, stratified flow may be of interest in conjunction with the behavior of the ECC in the cold leg of a PWR in small-break accidents. Further, a study of this flow configuration may provide an important addition to our understanding of the flocding process because of the relative simplicity and flexibility of the stratified flow. For nearly-horizontal countercurrent flooding, a modified Wallis parameter, J_{mk}^*, may be used as a dimensionless velocity scale, which considers the effect of inclination:

$$J_{mk}^* = j_k \left[\frac{\rho_k}{(\rho_f - \rho_g) g L \sin\theta} \right]^{1/2} \tag{1}$$

where the hydraulic diameter of the test section is chosen as the length scale, L, and j_k is the superficial velocity for the k-phase. This parameter represents the ratio of inertia force to gravity force and has emerged form the normalization of a combined form of momentum equations for gas and liquid phase in countercurrent flow[4]

In the present study, the flooding phenomenon and hysteresis effects in nearly-horizontal countercurrent stratified flow are investigated. Experimental data of the flooding velocity, liquid penetration rate, and critical vapor velocity both in steam/saturated-water flow and in steam/subcooled-water flow are presented and the condensation effect on these values is analyzed explicitly. Further, the initiation and basic mechanisms of hysteresis effects and flooding are discussed. Finally, a countercurrent flow regime map is constructed, which covers from a stable-operating region to a completely upwards cocurrent flow.

2. Experimental System and Procedure

The experimental apparatus is made up of a test section, two water storage tanks, heat exchanger, and two circulating pumps, as shown in Fig. 1. The test section is a square duct

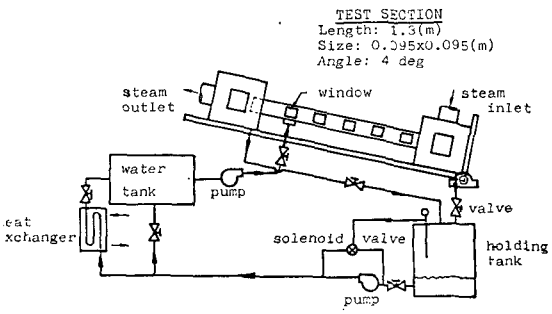

Fig. 1 Schematic diagram of experimental apparatus

approximately 1.3 m long with a size of 9.5 cm×9.5 cm. The test section has its own support system which permits any inclination between 0 and 90 degree, but has been fixed at 4 degree from the horizontal in the present study.

The water is introduced through a porous plate at the top portion of the test section and is drained in the lower chamber. Hot water discharged from the test section is collected in a holding tank whose water level is controlled by a bypass solenoid valve. The water inlet temperature can be regulated over the range of 7~98°C by varying the coolant rate in the heat exchanger.

The steam comes from the building supply, which is nominally saturated and at a pressure of 1.02 MPa. A moisture separator and throttling valve assure dry, superheated steam at the entrance to a manifold of flow measurement venturis with a diameter of either 3.18 cm or 5.08 cm. The absolute pressure and temperature are monitored at the venturis to determine the thermodynamic condition of the incoming steam. The steam has normally 10~40°C superheat at the entrance of the test section and was asumed to be at 1 atm pressure(0.1 MPa) for calculating its properties.

The temperatures of the steam and the water are measured with chromel-alumel thermocouples at the inlet and outlet. Pressure taps of 0.25 mm in diameter allow pressure drop measurement in order to detect the onset of flooding. The steam flow rate is calculated using the equation of state and the isentropic energy equation, based upon the measurement of thermodynamic state and pressure drop at the venturi. It showed agreement with the calibrated flow rate within an accuracy of ±2%. The signals from the thermocouples, transducers and flowmeters are processed by a PDP 11-34 computer interfaced with a multichannel A/D conveter.

The data of the onset of flooding were obtained by either increasing(flooding) or decreasing the steam flow rate(de-flooding) at fixed water inlet flow rates(water-first mode) and by increasing the water flow rate at fixed steam flow rates(steam-first mode) in order to investigate the effect of the operational mode. However, the water-first mode was chosen, for convenience, for the study of flow behaviors during the partial delivery stage. The onset of flooding was determined mainly by visual observations, but occasional checks by means of the pressure drop measurements were made to assure the reliability of the data. The penetration rate during the partial delivery stage was also monitored by guaging a rise of water level in the upper chamber in order to reveal the hysteresis effect in both condensing and non-condensing flows.

3. Results and Discussion

3.1. Intiation Mechanisms of Flooding

The data of the dimensionless vapor flooding velocity in steam/saturated-water are shown in Fig. 2. Three distinct methods of operation are indicated in the figure. The result shows that

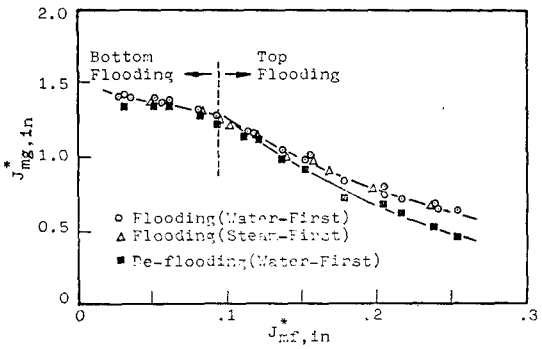

Fig. 2 A comparison of flooding and de-flooding velocities in steam/saturated-water flow

the flooding velocity in nearly-horizontal countercurrent flow is relatively insensitive to the method of operation whereas the deflooding point, which refers to the recovery point of a stable countercurrent flow when the steam flow rate is gradually decreased, lies slightly lower than the flooding point. This difference was also observed by several investigators[5,6] in vertical countercurrent flow. However, the deviation in the nearly-horizontal flow appears to be insignificant compared to that in the vertical flow.

It is also shown in Fig. 2 that the locus of the onset of flooding changes from the bottom of the test section to the top as the liquid injection rate increases over $J_{mf}^*=0.094$ approximately, resulting in two distinct slopes in the flooding curve. The transition may be also found in the literature for a vertical annular air-water flow.[7] This appears to be closely associated with the presence of a hydraulic jump at the liquid entrance. When $J_{mf}^*<0.094$, flooding was initiated at the bottom end of the tube after well-developed roll-waves have appeared on the gas-liquid interface. During the development of the flooding flow, a rough and thick liquid film was observed with formation of a liquid slug whose crest was as high as several times the mean film thickness. At the onset of flooding the water slug propagated backwards with significant entrainment of liquid droplets torn from the tips of the slug. In this region, therefore, flooding may be regarded as a limiting condition for countercurrent flow, which is retarded mainly by interfacial drag as described in Lee and Bankoff[8]. The tube-end effects on flooding process may be thought to be insignificant in the region. However, at high liquid injection rates($J_{mf}^*>0.094$), the onset of flooding took place in a quite different manner. A stationary liquid slug due to the effect of hydraulic jump appeared at the liquid entrance. The height of the slug grew due to the Bernoulli effect as the vapor velocity was increased. At a certain point, the upwards vapor flow started to shear off the crest of the slug, leading to the onset of flooding. Neither evident roll-wave nor significant entrainment was observed in this region and the initiation of flooding was basically governed by the liquid-entrance effect. Thus, a considerable reduction of the dimensionless vapor flooding velocities was indicated in this region, compared to those under an ideal liquid-entrance condition.

3.2. Condensation Effect

The influence of condensation on the onset of flooding may be considered in terms of both local and global effects. The local effect is associated with the change of the vapor flooding velocity due to local condensation heat transfer. However, this effect seems to be insignificant in most practical cases, as described in Lee and Bankoff[9]. On the other hand, considerations of the global effect focus on the calculation of the effective steam flow rate to initiate flooding. The effective steam flow rate is not, in general, equal to the steam supply rate, unless the locus of flooding is the bottom of the tube. If flooding is initiated at some

other location, the reduction of the steam flow rate due to condensation must be considered. This effect is of practical interest, particularly in conjunction with steam-water countercurrent flow in nuclear reactor safety systems.

Vapor flooding velocities in steam/subcooled-water flow are illustrated in Fig. 3. It is shown that a larger steam supply rate is needed to initiate flooding for a higher liquid subcooling in the top flooding region, compared to that in steam/saturated-water flow. The difference between adiabatic($T_{f,in}$=95°C) and condensing ($T_{f,in}$=60°C and 36°C) flooding curves in the figure represents the amount of steam condensed inside the tube. Thus, the global effect of condensation is important in determining the

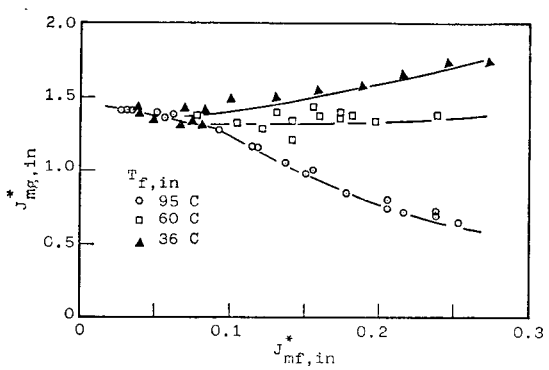

Fig. 3 Flooding velocities in steam/subcooled-water flow

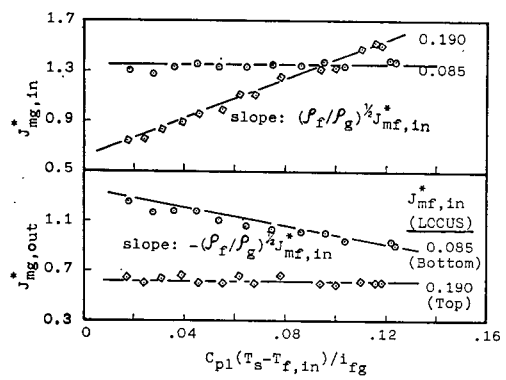

Fig. 4 A comparison of Dimensionless inlet and outlet vapor flooding velocities with variation of liquid subcooling

vapor flooding velocity for the top flooding. However, for the bottom flooding, this effect can be ignored, as shown in Fig. 4. A comparison between the dimensionless vapor inlet and outlet flooding velocity is illustrated in this figure for both top and bottom flooding. For the top flooding, the vapor outlet flooding velocity is almost constant regardless of the degree of liquid subcooling whereas so is the vapor inlet flooding velocity for the bottom flooding. Thus, the dimensionless effective steam velocity may be written as

$$J^*_{mg,e}=J^*_{mg,in}-\eta\cdot f\cdot Ja\cdot J^*_{mf,in} \quad (2)$$

where η is the dimensionless parameter, which has a value of 1 for top flooding cases and 0 for bottom flooding cases, and f is the condensation efficiency. If the initiation of flooding takes place in the middle of the test section, η should have a value between 0 and 1. However, this is unlikely because the locus of the initiation is largely dependent upon the tube-end geometry. In Equation (2), Ja is the Jacob number, defined as;

$$Ja=(\rho_f/\rho_g)^{1/2}[C_{pl}(T_s-T_f)/i_{fg}] \quad (3)$$

where C_{pl} is the liquid heat capacity and i_{fg} is the latent heat.

The critical gas velocity, which refers to the vapor velocity at the inception of a hanging film, was monitored for various liquid subcoo-

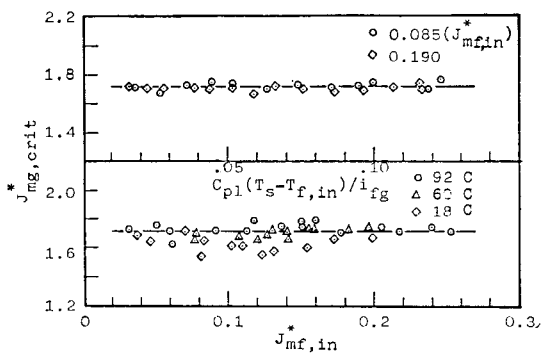

Fig. 5 Critical vapor velocities with variation of liquid subcooling and liquid injection rate

lings as well as liquid injection rates, as shown in Fig. 5. It is indicated that the critical velocity is independent of both the liquid injection rate and the degree of liquid subcooling in nearly-horizontal flow. The irrelevance of the critical gas velocity to the liquid injection rate coincides well with the results of vertical adiabatic flow tests made by several investigators[10,11]. One notes that it may reflect a possibility of the exitence of hysteresis effects during the partial delivery stage because the relation between the partial delivery rate and the upwards steam flow rate is unique, regardless of the liquid injection rate and the condensation rate.

3.3. Mechanisms of Hysteresis Effects

As mentioned above, hysteresis effects refer to a sudden reduction of the liquid delivery rate immediately after flooding is initiated as the steam flow rate is increased. These may take place either due to condensation or due to the breakup of a liquid film. In an effort to uncover their mechanisms, the liquid penetration rates both in steam/saturated-water flow and in steam/subcooled-water flow were measured for several liquid injection rates, as shown in Fig. 6. It is noted that the hysteresis effects evidently exist in condensing flows. Visual observation showed an abrupt burst of the liquid film flow once flooding has been initiated, leading to a sudden reduction of penetration rate. The mechanism of these hysteresis effects may be described as follows. At the onset of flooding, a portion of the liquid flow is carried upwards by the steam flow and thus, the liquid downwards flow rate is reduced. This, in turn, decreases an overall condensation rate, resulting in a subsequent increase of the effective steam flow rate. It now acts to bring more liquid upwards, leading to a further decrease of the overall condensation rate. This process will be repeated itself until a stable partial delivery is made. However, it will take place very rapidly, so that the sudden reduction of the liquid penetration rate will be observed. The hysteresis observed by Liu and Collier[12] for a vertical annular condensing flow may occur on this mechanism. From this description, one may note that the hysteresis effect always take place in a condensing flow if flooding is initiated at the top of the tube as in the present case. The hysteresis effect may also exist in non-condensing flow, as found in the works of Clift, et al[6] and Wallis, et al.[3] This may take place probably due to the breakup of a liquid film and thus their mechanism should be distinguished from the one described above because no condensation is involved. Their possible mechanisms and initiation conditions are proposed elsewhere[13].

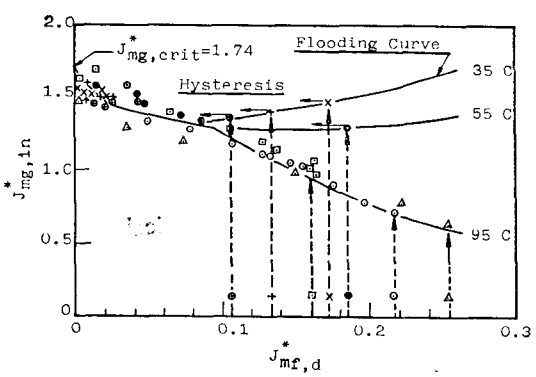

Fig. 6 Hysteresis effects during partial delivery

3.4. Countercurrent Flow Regime Map

A countercurrent flow regime map in nearly-horizontal flow has been constructed, as shown in Fig. 7. Four distinct boundaries are indicated: maximum 100% penetration(Boundary A), transition to the slug flow(Boundary B), minimum 0% penetration(Boundary C), and transition to the complete upwards occurrent flow

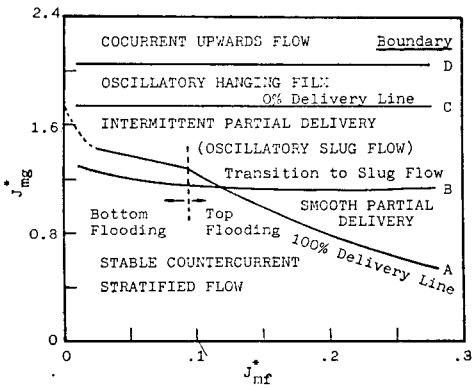

Fig. 7 A Countercurrent flow regime map for nearly-horizontal steam/saturated-water flow

(Boundary D). Below the flooding curve(Boundary A), a stable countercurrent stratified flow is maintained although the interface exhibits various wave patterns, such as two-and three-dimensional wave and roll wave. The roll-waves superimposed on the three-dimentional waves, however, appear only in the bottom flooding region. The region between boundary A and B in the bottom flooding case corresponds to a slug flow, which is a preliminary stage to the initation of flooding under an ideal liquid entrance condition. In the top flooding case, this region represents a stable partial delivery of the liquid. Beyond the boundary *B*, an oscillatory and transient plug flow is developed with an intermittent partial delivery. At the boundary $C(J_{mg}^*=1.74)$, a hanging film with an attachment point at the bottom of the tube appears and thus the net delivery rate becomes zero. Between the boundary *C* and *D*, an oscillatory hanging film is observed with the attachment point moving upwards along the channel wall as the steam flow rate is increased. Finally, when it reaches the liquid entrance, a complete cocurrent upwards two-phase flow is developed. This transition takes place at $J_{mg}^*=2.05$ in the present test section, regardless of the liquid injection rate and the degree of liquid subcooling.

4. Conclusions

A countercurrent flow regime map has been developed in a nearly-horizontal stratified two-phase flow. It shows four distinct transitions, including maximum 100% liquid penetration, a transition to the slug flow, minimum 0% liquid penetration, and a transition to the complete cocurrent upwards flow, The influence of condensation on these transitions have been investigated, indicating only the 100% penetration line moves upwards substantially in the $(J^*_{mg,in}, J^*_{mf,in})$ plane due to the global effect. The critical vapor velocity is independent of the liquid subcooling as well as the liquid injection rate.

The global effect of condensation in the top flooding also gives rise to hysteresis effects during the partial delivery stage, whose initiating mechanism has been proposed. From this postulation, one may conclude that the hysteresis effects always exist due to condensation only if flooding is initiated at the liquid entrance.

Finally, the onset of flooding is unaffected by condensation in bottom flooding cases, indicating that the flooding velocity in the steam-water flow may be predicted from the experimental results of non-condensing flow such as air-water flow. However, for top flooding cases, the effective steam velocity should be used instead of the steam inlet velocity in determining the vapor flooding velocity. Therefore, for practical purposes, further studies are suggested on the criteria of the occurrence of the top and bottom flooding in various geometrical conditions of interest.

Acknowledgement

The author appreciates financial support from the

Ministry of Education of Korea during the course of this study.

References

(1) S.G. Bankoff and S.C. Lee, "A Brief Review of Countercurrent Flooding Models Applicable to PWR Geometries," Nuclear Safety Journal, in press

(2) C.L. Tien and C.P. Liu, Survey on Vertical Two-Phase Countercurrent Flooding, EPRI Report NP-984, 1979

(3) G.B. Wallis, D.C. de Sieyes, R.J. Rosselli, and J. Lacombe, Countercurrent Annular Flow Regimes for Steam and Subcooled Water in a Vertical Tube, EPRI Report NP-1336, 1980

(4) S.C. Lee and S.G. Bankoff, "Stability of Steam-Water Countercurrent Flow in an Inclined Channel: I. Flooding," ASME J. Heat Transfer, Vol. 105, pp. 713~718, 1983

(5) G.B. Wallis, One-Dimensional Two-Phase Flow, Chap. 11, p. 340, McGraw-Hill, New York, 1969

(6) R. Clift, C.L. Pritchard, and R.M. Nedderman, "The Effect of Viscosity on the Flooding Conditions in Wetted Wall Columns," Chemical Engineering Science, Vol. 21, pp. 87~95, 1966

(7) G.L. Shiers and A.R. Pickering, "The Flooding Phenomenon in Countercurrent Two-Phase Flow," Proceedings of the Symposium on Two-Phase Flow, Vol. 2, pp. B 501~B 538, University of Exeter, England, 1965

(8) S.G. Bankoff and S.C. Lee, "A Critical Review of the Flooding Literature," Multiphase Science and Technology(G.F. Hewitt, J.M. Delhaye and N. Zuber eds.), Vol. 2, Hemisphere Publishing Co., Washington, D.C., U.S.A, in press

(9) S.C. Lee and S.G. Bankoff, "Parametric Effects on the Onset of Flooding in Flat-Plate Geometries," International Journal of Heat and Mass Transfer, Vol. 27, pp. 1691~1700, 1984

(10) O.L. Pushkina and Y.L. Sorokin, "Breakdown of Liquid Film Motion in Vertical Tubes," Heat Transfer-Soviet Research, Vol. 1, pp. 56~64, 1969

(11) G.B. Wallis and S. Makkenchery, "The Hanging Film Phenomenon in Vertical Annular Two-Phase Flow," ASME J. Fluids Engineering, Vol. 96, pp. 297~298, 1974

(12) J.S.K. Liu and R.P. Collier, "Heat Transfer in Vertical Countercurrent Steam-Water Flooding Flows," Proceeding of the ASME Symposium on Basic Mechanisms in Two-Phase Flow and Heat Transfer, New York, N.Y., U.S.A. 1980

(13) S.C. Lee and S.G. Bankoff, "Flooding and Hysteresis Effects in Countercurrent Steam-Water Flow," submitted for publication in AIChE J., 1984